Article

Experimental Study of Coaxial Jets Mixing Enhancement Using Synthetic Jets

Binglong Zhang, He Liu *, Yangyang Li, Hui Liu and Jinzhong Dong

School of Energy and Power Engineering, Beihang University, Beijing 100191, China; zgbglg@buaa.edu.cn (B.Z.); zy1904413@buaa.edu.cn (Y.L.); liuhui_0105@163.com (H.L.); DD309@buaa.edu.cn (J.D.)
* Correspondence: liu_he5656@buaa.edu.cn

Abstract: Synthetic jets perpendicular to the mainstream have been used to experimentally study the coaxial jets mixing enhancement in this paper. The parameters of coaxial jets such as vorticity, streamwise velocity, radial velocity, Reynolds shear stress, and turbulence intensity are measured using the particle image velocimetry (PIV) and hot wire anemometers. The distribution characteristics of these parameters with and without synthetic jets were obtained. The mechanism of coaxial jets mixing enhancement using synthetic jets was summarized by analyzing these experimental results, and it was also found that the momentum coefficient was the most critical factor for jets mixing enhancement. The comparative experiments fully verified the mechanism, showing that with an appropriate momentum coefficient, the synthetic jets significantly enhanced coaxial jets mixing.

Keywords: synthetic jet; jet mixing enhancement; momentum coefficient; streamwise vortices

1. Introduction

Jet mixing enhancement is widely used in many industries, such as the energy industry, chemical reactions, and especially in the aerospace field. For example, enhancing the mixing of air and fuel in the combustion chamber to improve emission quality [1]. Jet mixing enhancement is applied to aero engines to achieve thrust augmentation [2] and adjusting infrared radiation visibility [3]. Jet mixing enhancement methods can be divided into two categories: Active flow control technology and passive flow control technology. Solid tabs [4], chevron nozzles [5], lobe nozzles [6], and other methods to modify the nozzle geometry to control the flow are called passive flow control technology. Synthetic jets [7–10], plasma actuators [11,12], acoustic actuation [13], control jets [14,15], and pulsed jets [16] generally input additional or auxiliary energy into the flow belonging to active flow control technology.

Active flow control technology has many significant advantages. It can adjust control parameters according to flow conditions and turn off when it is not needed. Therefore, active flow control technology can achieve higher performance on jet mixing enhancement. Smith et al. [17] numerically studied jet mixing enhancement with pulsed jet. The simulations were in good agreement with the experimental data, showing that the jet potential core lengths at several conditions were significantly shortened by pulsed jet. Zhou et al. [18] used two steady minijets to enhance a turbulent jet mixing. The flow field was measured by the flow visualization and hot wire technique to explore the physical mechanism of mixing enhancement. They found that periodical structures generated by minijets significantly affected the development of the main jet. Kamran et al. [19] studied the mixing enhancement of a transonic jet using steady and pulsed control jets separately. They found that the control jet can effectively enhance the mixing and the potential core length can be shortened by 50% in the experiment. The interaction area between the jet and ambient was a key factor in the physical processes of mixing. The unsteady pulsed jet had a better effect on mixing than the steady jet.

The synthetic jet is one of the most promising applications in active flow control technology and has received widespread attention [20–23]. Synthetic jets do not require additional air and pipelines, and are also known as zero-mass jets. Scholars have used synthetic jets to study jet mixing enhancement in many application fields, proposing the main mechanisms of synthetic jet mixing enhancement in their respective research fields. Chen et al. [24] investigated the synthetic jet to improve fuel mixing in combustion chambers. The temperature and velocity distributions were measured to indicate that mixing was significantly enhanced by synthetic jets. Wang and Menon [25] performed a series of numerical simulations on fuel and air mixing enhancement using synthetic jets. They analyzed the fuel velocity and species distribution, finding that synthetic jets perpendicular to the fuel jet enhanced jet mixing more significantly than synthetic jets parallel to the fuel jet. Chiekh et al. [26] experimentally studied the control of the diffuser flow with two synthetic jets placed at the entrance. They found that a high vorticity zone was generated when only one synthetic jet worked, which enhanced mixing and increased the jet deflection angle. When two symmetrically placed synthetic jets worked, the mixing enhancement was more obvious, and the flow section significantly increased. Tamburello et al. [27] experimentally studied the interaction between a synthetic jet and a free jet (Re = 6600). They analyzed the control mechanism by changing parameters such as Strouhal numbers, the direction angle of synthetic jet, and the momentum coefficients. Results showed that mixing was enhanced appreciably by the synthetic jet. The increase of the synthetic jet momentum coefficient can increase its penetration depth and enhance the strength of vertical structures. The synthetic jet achieved the most significant effect on mixing when the Strouhal number was 0.32 under low momentum coefficient condition. However, the effect of the Strouhal number on mixing was not obvious with high momentum coefficient. Eri et al. [28] investigated the mixing enhancement of subsonic round jet using high-momentum synthetic jets. They numerically simulated the temperature reduction of the mainstream affected by synthetic jet penetration depth, vorticity of vortices pair, and interaction area. Results showed that synthetic jets reduced the length of the high temperature region by 75%. The streamwise vortices were the major mixing mechanism, which improved heat and mass transfer between the mainstream and ambient. Mainstream flapping was the second mechanism. Hong et al. [29] used numerical simulation methods to study the mixing enhancement of heat temperature jet using piston-type synthetic jets. They found that the primary jet flapping caused by the synthetic jet accelerated the spread of potential core fluid to the environment. The streamwise vortex increased the quality of ambient and primary jet potential core transportation. The low-temperature zone in the potential core changed positions under the action of the synthetic jet, which promoted the mixing of ambient and primary jet. They named this phenomena as geometric axis transformation. Based on their results, it can be seen that jet flapping, streamwise vortex, and geometric axis transformation are the main mechanisms of jet mixing enhancement.

Coaxial jets mixing enhancement is more complicated and has a wide range of applications. Especially in the aerospace field, mixing enhancement of combustion gas and air from a rear variable area bypass injector in the variable cycle engine can adjust infrared radiation visibility and augment thrust. Mixing enhancement of fuel air and oxygen in air-breathing rocket engine or ramjet engine can significantly improve its combustion efficiency. Coaxial jets are not only mixed with the ambient air, but the two jets inside and outside are also mixed. Davis, Glezer [30], and Ritchie et al. [31] used nine synthetic jet actuators parallel to the mainstream to investigate mixing processes in the shear layers of coaxial jets with experimental methods. The hot wire anemometry and planar laser-induced fluorescence were used to measure the structure and scalar concentration of mixing fields under three velocity ratio conditions. Results showed that synthetic jets caused the mainstream to expand in the radial direction and the vortical structure between inner and outer jet increased. The continuous high frequency synthetic jets resulted in the enhancement of small-scale mixing in the flow field near outlet, which greatly increased the radial velocity of mainstream. The low frequency amplitude modulation of synthetic jets generated large-

scale vortical structures which enhanced the radial flow toward the mainstream centerline. Liu et al. [32] numerically studied the coaxial jets mixing enhancement with synthetic jets. The effects of different phases between two synthetic jets were studied, and it was found that mixing enhancement was significant when the phase angle was greater than zero and less than a maximum value.

There have been many studies on the mixing enhancement of free jets and ambient air, but few have specialized in coaxial jets mixing enhancement. In this paper, experimental methods were used to study the distribution of parameters such as velocity, Reynolds shear stress, and turbulence intensity in the coaxial jet with and without synthetic jets perpendicular to the mainstream. Then a series of comparative experiments were carried out to explore the mechanism and key factors of coaxial jets mixing enhancement with synthetic jets.

2. The Experimental Method

In the experiment, the synthetic jet actuators were evenly placed at the coaxial jet nozzle outlet, and the synthetic jets were perpendicular to the nozzle jet. In the measurement coordinate system, the origin was the nozzle outlet center point. The X-axis coincided with the nozzle symmetry axis, and its positive direction was the same as the mainstream. The Y-axis ran along the nozzle outlet radial direction, which was perpendicular to the mainstream.

2.1. The Coaxial Jet Nozzles

Two coaxial jet nozzles were used in the experiment, and the dimensions are shown in Table 1. The central jet was ejected from the inner duct, and the annular jet was ejected from the outer duct. The air of nozzle jet was provided by the wind tunnel. The inner duct outlet diameter of the nozzle was represented by D_i, the outlet velocity was U_i, and the Reynolds number there was 13,000. The outer duct outlet diameter was D_o, and the outlet velocity was U_o. The structure of nozzle A and the combined actuators disk is shown in Figure 1. Nozzle B had a similar structure as nozzle A, except that the outer duct diameter was smaller.

Table 1. Parameters of nozzles and synthetic jet actuators.

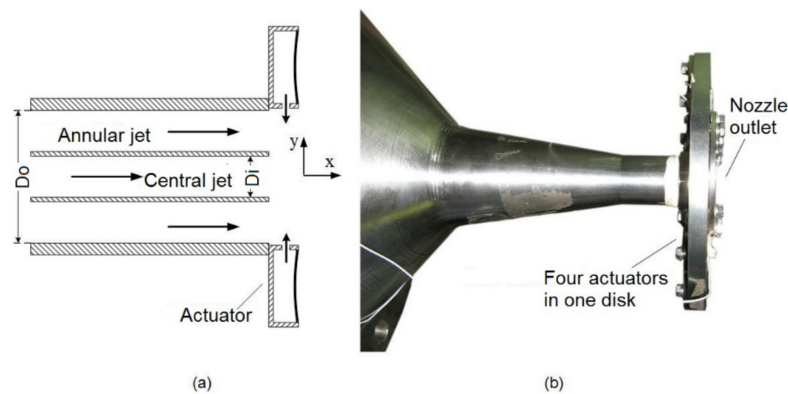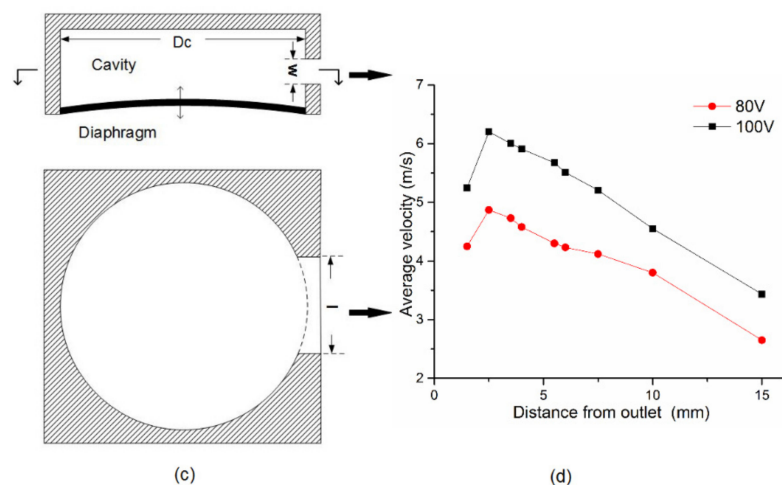| Case	Nozzle	D_i (mm)	D_o (mm)	U_i (m/s)	U_o (m/s)	Re_i 10^4	n	U_s (m/s)	C (%)
1	Nozzle A	10	50	20 ± 0.21	10 ± 0.16	1.3	4	5 ± 0.11	0.45
2	Nozzle B	10	25	20 ± 0.21	10 ± 0.19	1.3	4	5 ± 0.11	1.38
3	Nozzle A	10	50	20 ± 0.21	10 ± 0.16	1.3	12	5 ± 0.11	1.36
4	Nozzle A	10	50	20 ± 0.21	10 ± 0.16	1.3	4	9 ± 0.14	1.47

Figure 1. *Cont.*

Figure 1. Schematic diagram (**a**) and installation photograph (**b**) of nozzle and actuators, actuator structure diagram (**c**), and actuator outlet centerline velocity distribution (**d**).

2.2. The Synthetic Jet Actuators

The diaphragm type piezoelectric ceramic synthetic jet actuator was used in the experiment, which converted electric energy into diaphragm vibration kinetic energy, and then periodically induced the synthetic jet. It had the advantages of simple structure, light weight and convenient control. The structure of the actuator is shown in Figure 1a. Round copper with a thickness of 0.1 mm and a diameter of 50 mm was used as the diaphragm. The piezoelectric ceramics on the diaphragm had a thickness of 0.2 mm and a diameter of 35 mm. The diaphragm frequency used in the experiment was 310 Hz. The outlet size was 0.5 mm × 20 mm. The average velocity distribution on the outlet centerline of the actuator is shown in Figure 1d. The highest velocity on the centerline was reached at a distance of 3 mm from the outlet. This velocity was used to represent the actuator outlet velocity, denoted by U_s. For actuators whose diaphragm material, geometric structure, and diaphragm frequency were already determined, different velocities at the outlet were obtained by adjusting the diaphragm voltage. Before the experiment, through constant attempts, the diaphragm voltage corresponding to the outlet velocity in every case were found.

Four identical actuators were evenly mounted on a circular disk with an inner diameter equal to the nozzle outer diameter to form a combined actuators disk. Since two different outer diameter nozzles were used in the experiment, there were also two types of combined actuators disks, but the actuators inside them were the same. The disk was installed at the outlet of the nozzle. The synthetic jets of these actuators were perpendicular to the nozzle jet and worked in the same phase to prevent mainstream deflection. The number of actuators used in comparison experiments is represented by *n* in Table 1.

2.3. The Measuring Devices

In the experiment, the IFA300 hot wire anemometer produced by TSI measured the velocity related data for each position under the control of the traverse measurement system, then the average velocity, streamwise velocity, radial velocity, and turbulence intensity of mainstream were all analyzed. The sampling frequency was 10,000 times per second, and the error of the experimental system with hotwire measurements is 2.3%. The velocity signal was sampled and recorded by the data processing unit.

The TSI particle image velocimetry (PIV) system with a double-pulse Nd: YAG 120 mJ/pulse was used to monitor and acquire the velocity field. Atomized ethylene glycol was used as a tracer particle. The velocity and vorticity distribution in the range of 80 mm × 100 mm in the X-Y plane near the nozzle outlet were continuously collected. Experimental errors were mainly from the probe calibration error, measuring error and mea-

suring position error. The Maximum experimental error with PIV system were controlled within ±0.2 m/s.

Distribution parameters for nozzle A with and without actuators were first measured in the experiment, and the characteristics of the coaxial jets mixing flow field with and without synthetic jets were obtained respectively. Then, a series of comparative experiments were carried out to analyze the mechanism and key factors of coaxial jets mixing enhancement with synthetic jets.

3. Results and Discussion

3.1. The Parameter Distribution of Coaxial Jets

Unlike conventional jet, the coaxial jet flow field has two shear layers. The shear layer where the central jet and the annular jet are mixed is called the inner shear layer, and the shear layer where the annular jet is mixed with ambient air is referred to as the outer shear layer.

3.1.1. Velocity and Vorticity

Figures 2–5 present the experimental results for the flow field of nozzle A in case 1. It can be clearly seen from Figure 2a,b that under the influence of the actuators, both the inner and outer shear layers become thicker with the development of the flow, and the velocity gradient becomes smaller along the radial direction. In order to facilitate the comparison between different cases, the distance from the position of the central jet with 16 m/s to the inner duct outlet was defined as the length of the potential core, which is 90 mm in Figure 2a.
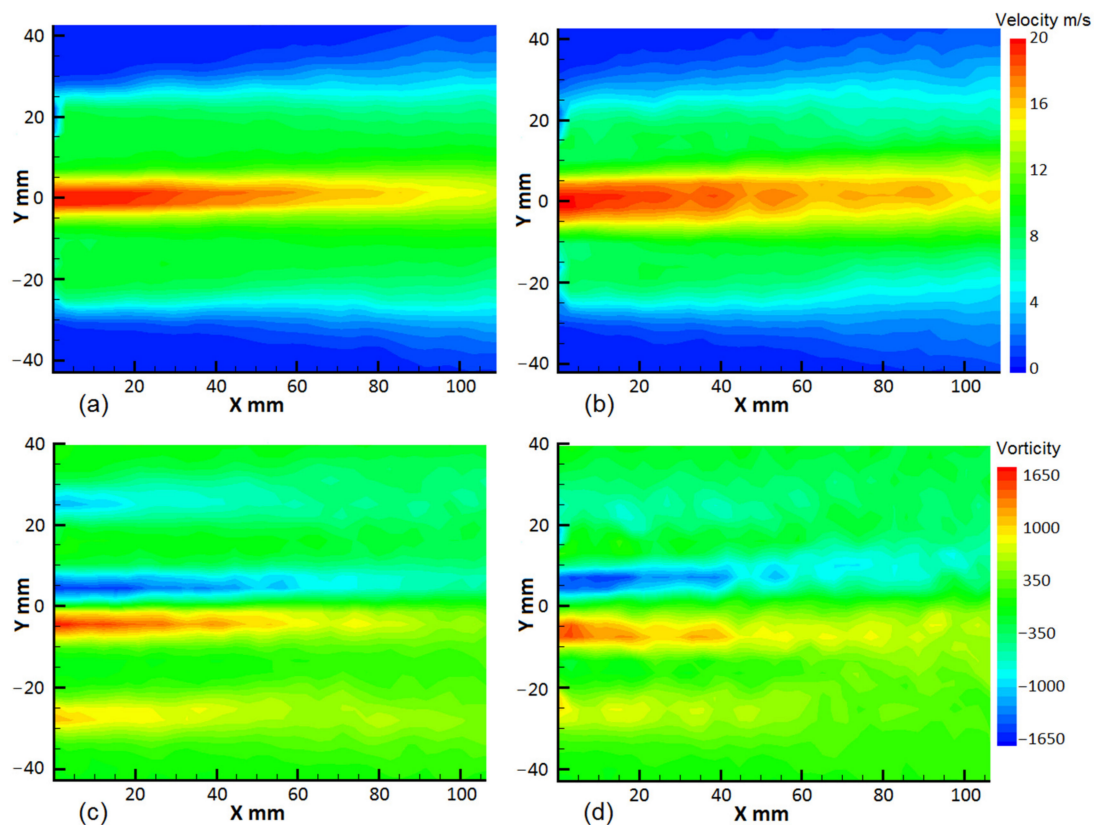
Figure 2. Time average velocity (**a**,**b**) and vorticity (**c**,**d**) distribution of nozzle A without (**a**,**c**) and with (**b**,**d**) actuators.
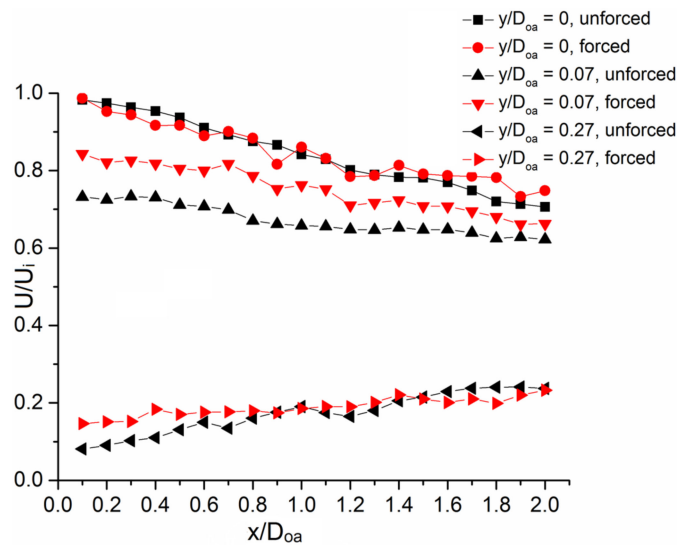
Figure 3. Velocity distribution along axial direction at different sections of nozzle A.
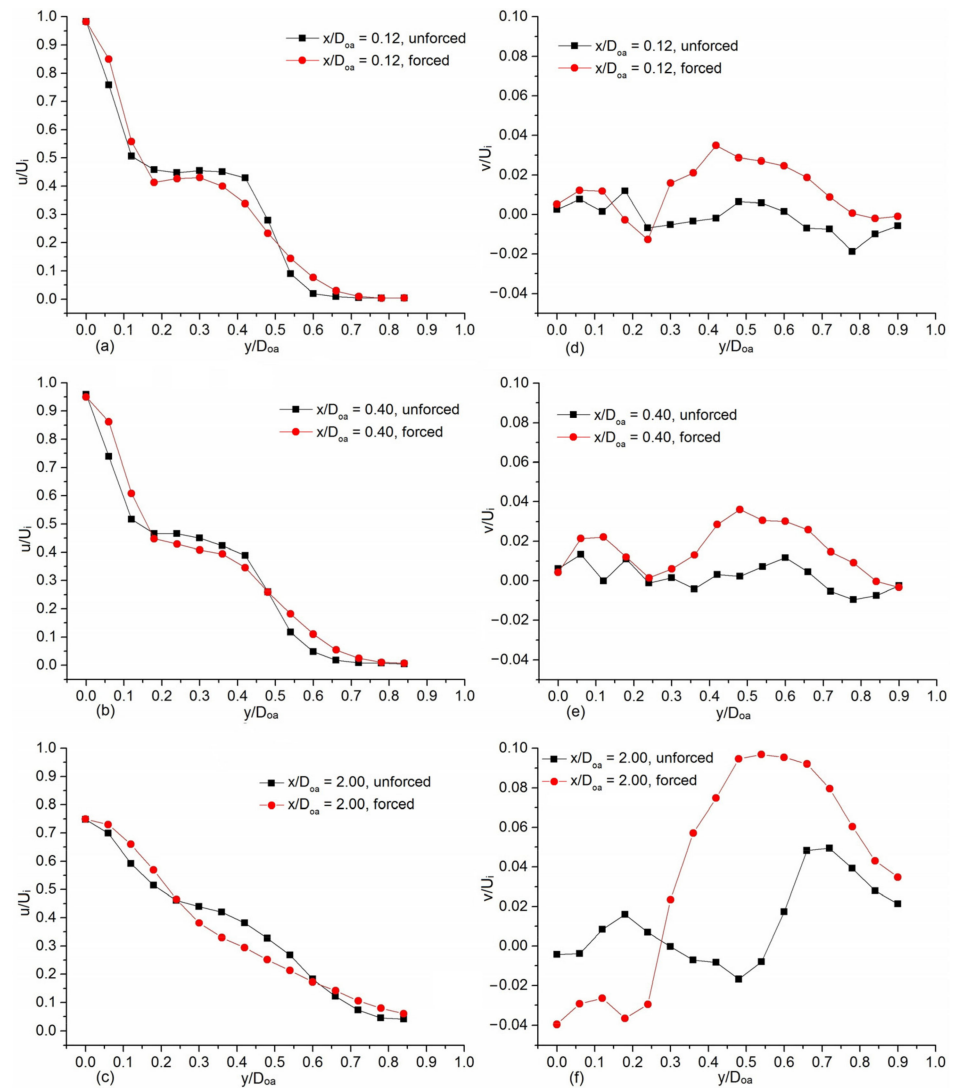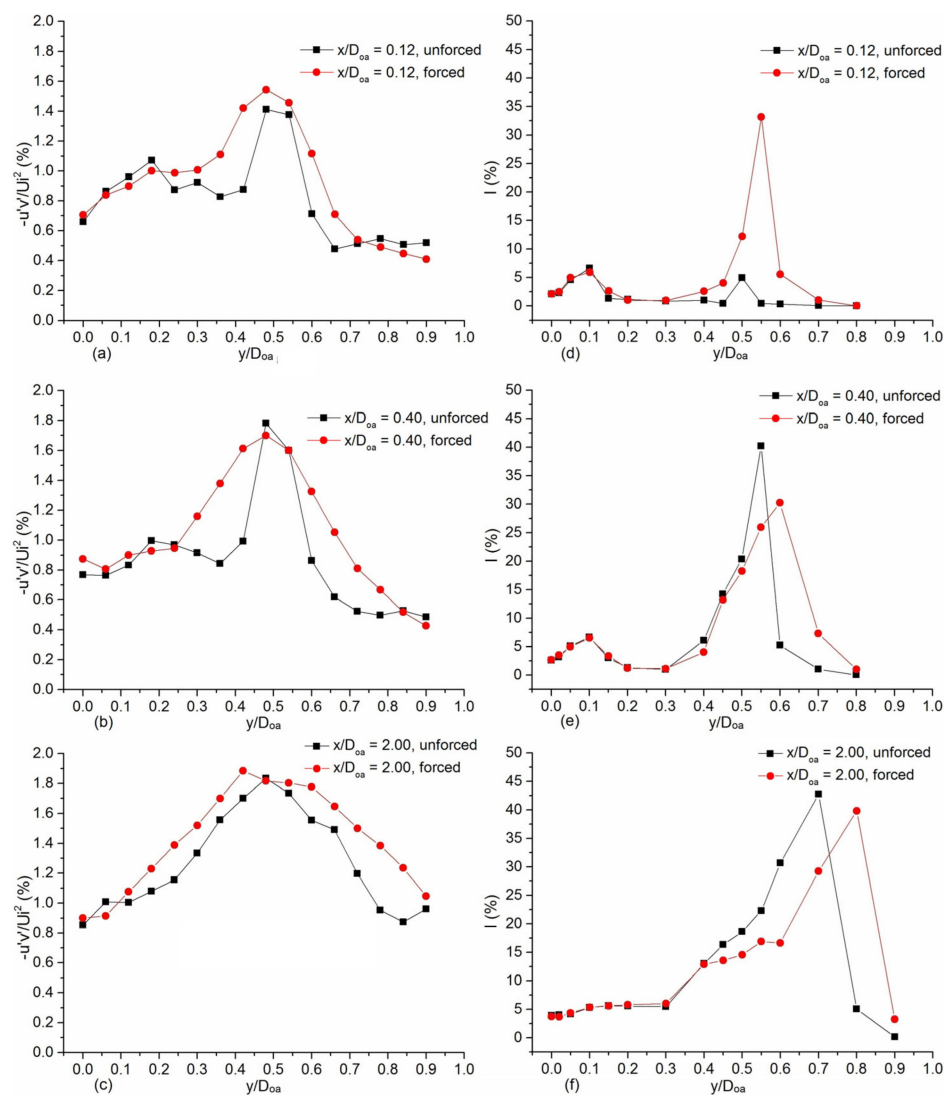

Figure 4. The radial distribution of time averaged streamwise velocity (**a**–**c**) and radial velocity (**d**–**f**) at different axial positions of nozzle A.

Figure 5. The radial distribution of Reynolds shear stress (**a–c**) and turbulence intensity (**d–f**) at different axial positions of nozzle A.

Vorticity is mainly distributed in the shear layer. It can be clearly seen in Figure 2c that the coaxial jet has two major vortices, and the vorticity of vortices in the inner shear layer is more concentrated. Davis [27] named it the primary vortices, and named another in the outer shear layer as the secondary vortices. In Figure 2d, the vorticity showed significant diffusion along the axial and radial directions, indicating that the influence of the vortices expanded and more air from jets and ambient entered the shear layers to mix.

In order to study the effect of the synthetic jet on the shear layer, three positions were selected on the X-Y plane in the radial direction, and the velocity distribution along the axial direction was measured. In Figure 3, $y/D_{oa} = 0$ was the center of the nozzle, the velocity value did not change significantly with actuators as a whole, indicating that the airflow at the center was not directly affected by the synthetic jet. $y/D_{oa} = 0.07$ was located in the inner shear layer. The velocity curve slightly fluctuated and the value in the entire section improved by actuators, with an average increase of 11%. This is because more high velocity air from the central jet was entrained into the inner shear layer, causing its disturbance to increase. $y/D_{oa} = 0.54$ was located in the outer shear layer, the actuators increase the upstream velocity and reduce the downstream velocity. This indicates that the annular jet expanded radially in the upstream and more ambient air was entrained into the outer shear layer at downstream by synthetic jets, which enhanced the mixing of the annular jet and the ambient air.

3.1.2. Streamwise Velocity and Radial Velocity

Because of the axial symmetry of coaxial jets, only parameters distribution on the positive Y-axis are shown in Figures 4 and 5. The radial distribution of the dimensionless time averaged streamwise velocity at different axial positions is shown in Figure 4a–c. At x/D_{oa} = 0.12, the inner and outer shear layers were thin, and the velocity difference in layers was great, so the velocity gradient was large, and the slope of the curve in the region of two shear layers was steep. However, the velocity of the annular jet between two shear layers was relatively stable, so the curve there was straight. With the development of the mainstream, the shear layers became thicker and the straight section became smaller. Under the influence of actuators, the length of the straight section rapidly shortened and disappeared at x/D_{oa} = 2. A similar change occurred at these three positions after the actuators are turned on: In the radial direction, the streamwise velocity rose in the inner shear layer, then decreased on the inside of the outer shear layer and increased on the outside. These trends and the velocity distribution in Figure 3 were mutually evidenced, showing the characteristics of the flow field in the inner and outer shear layers being affected by synthetic jets.

The radial distribution of the dimensionless time averaged radial velocity at different axial positions is shown in Figure 4d–f. The radial velocity represented the radial penetration capability of the jet. Although the synthetic jet moved toward the center of the coaxial jets, it affected the mainstream to spread radially outward. At the positions corresponding to the inner and outer shear layers, the distribution of radial velocity exhibit a "peak-valley" shape, consistent with the counter-rotating vortex pairs. As the streamwise vortices dissipate along the axial direction, the radial velocity value continuously accelerated. Therefore, the "peak-valley" shape moved outward in the radial direction, and the shape amplitude became larger. After the actuators were turned on, the synthetic jets increased the streamwise vortices intensity, so the "peak-valley" shape amplitude at each selected position was significantly increased, especially near the outer shear layer. This means that the mainstream radial expansion capability was increased greatly by the synthetic jet, and the internal radial mixing was enhanced.

3.1.3. Reynolds Shear Stress and Turbulence Intensity

The Reynolds shear stress corresponds to the momentum exchange caused by the pulsation of fluid particles. For convenience, the simplified instantaneous Reynolds shear stress expression was $-u'v'$. The radial distribution of the dimensionless Reynolds shear stress is shown in Figure 5a–c. At x/D_{oa} = 0.12, the position of the left peak of the Reynolds shear stress curve corresponded to the boundary between the central jet and the annular jet, and the right peak corresponded to the boundary between the annular jet and the ambient air, indicating that the momentum exchange there was large. With the development of the mainstream, the inner shear layer expands outward and the velocity gradient became smaller, and the momentum exchange in the layer was at a similar level, so the left peak tended to be flat (x/D_{oa} = 0.4, x/D_{oa} = 2). After the actuators were turned on, the curves around the two peaks flattened and the span became larger. This was because the shear layer thickened, the velocity gradient became smaller, and the mainstream momentum exchange range expanded, indicating that the mixing of the jets here was enhanced. This change was more obvious in the left peak at x/D_{oa} = 0.12.

The turbulence intensity is the ratio of the root mean square of the velocity fluctuation to the time average velocity. Similar to the Reynolds shear stress distribution above, the turbulent intensity curve in Figure 5d also has two peaks at x/D_{oa} = 0.12, indicating that the velocity pulsations there were large. Since the inner shear layer velocity gradient gradually decreased in the axial direction, the left peak of the turbulence intensity became flat, which can be seen in Figure 5e,f. At the same time, the time average velocity of the outer shear layer reduced, so the right peak became larger (x/D_{oa} = 0.4, x/D_{oa} = 2). After the actuators were turned on, the right peak at x/D_{oa} = 0.12 increased significantly, i.e., by 7 times. This shows that synthetic jets cause velocity pulsation in the outer shear

layer to become more intense. At the same time, the velocity pulsation in the inner shear layer also increased, but since the time average velocity significantly increased (Figure 3, y/D_{oa} = 0.07), the left peak of the turbulence intensity barely changed.

3.1.4. Analysis of Parameter Distribution Results

The above results show the characteristics of flow field for coaxial jet nozzle A. The streamwise velocity gradient was large in the two shear layers, but the velocity of annular jet between the layers was relatively stable in the radial direction. The distribution of radial velocity in shear layers was in accordance with the streamwise vortices, showing a "peak-valley" shape. Both the Reynolds shear stress and the turbulence intensity showed two peaks on the radial distribution curve. The peak in the inner shear layer became flat with the development of mixing in the axial direction.

After the actuators were turned on, the vortex pairs formed at the outlet of actuators entered the shear layer with the synthetic jet, enhancing the development of streamwise vortices in shear layers. The primary and secondary vortices both expanded the influence region, and the inner and outer shear layers became thicker. The streamwise velocity rose in the inner shear layer, then decreased on the inside of the outer shear layer and increased on the outside. The radial velocity significantly increased, indicating that the radial penetration and mixing between jets is enhanced. Because the velocity gradient became smaller and the mainstream momentum exchange range expanded, the Reynolds shear stress curve around the two peaks flattened and the span became larger. The synthetic jets caused the velocity pulsation in the outer shear layer to become intense, so the turbulence intensity increased significantly. The distribution and change of the above parameters indicated that the synthetic jets effectively enhanced the coaxial jets mixing and shortened the time and space required for mixing. This is of great significance for practical applications.

3.2. Analysis of Comparative Experiments

Figure 6a,b show the velocity distribution of nozzle B without and with actuators in case 2. The length of the potential core in the original flow field was 50 mm. The central jet and the annular jet reached the same velocity at approximately x = 90 mm axially, and it can be considered that the two jets were fully mixed. After the actuators were turned on, the potential core length was reduced to 15 mm, and the two jets were fully mixed at x = 45 mm. The outer shear layer was significantly thicker and the velocity gradient was significantly smaller in the radial direction.
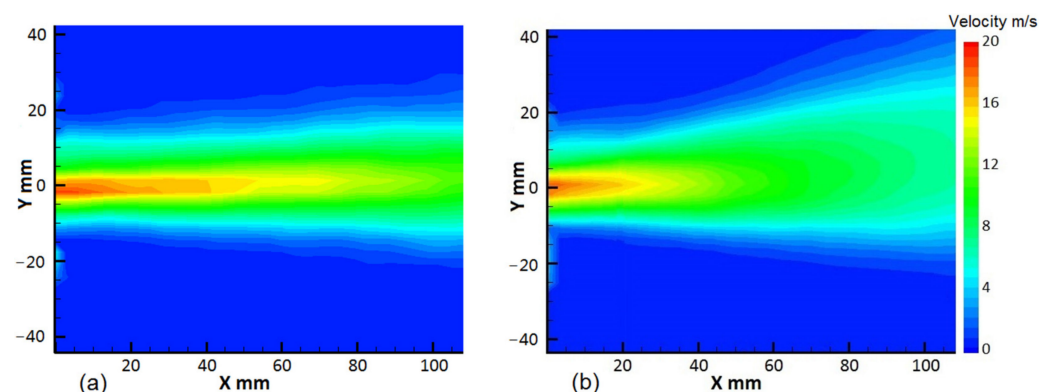
Figure 6. Time average velocity distribution of nozzle B without (**a**) and with (**b**) actuators.

It is apparent that the synthetic jets enhanced the jet mixing of nozzle B more significantly than nozzle A. The two nozzles had different annular outlet areas, and all other conditions are the same. The biggest difference between the experimental conditions of the two nozzles was the momentum coefficient. The momentum coefficient was the ratio of synthetic jets momentum to the coaxial jets momentum, which is represented by C in Table 1.

For nozzle A, the streamwise vortices caused the air inside the inner shear layer to move radially outward, and the high velocity air of the central jet fills into the shear layer, so that the velocity at $y/D_{oa} = 0.07$ inside the inner shear layer significantly increased (Figure 3). For nozzle B, the streamwise vortices affected the mainstream center. The center jet air was entrained outward by the streamwise vortices while the annular jet air was entrained inward, and the mixing is greatly enhanced. As a result, the central jet velocity was lowered, and the velocity inside the annular jet was increased. Similar mixing and velocity changes also occurred in the outer shear layer. Therefore, the velocity at $y/D_{oa} = 0$ and $y/D_{oa} = 0.07$ in the central jet range rapidly reduced under larger pulsations, and the velocity at $y/D_{oa} = 0.27$ in the outer shear layer slightly increased (Figure 7).
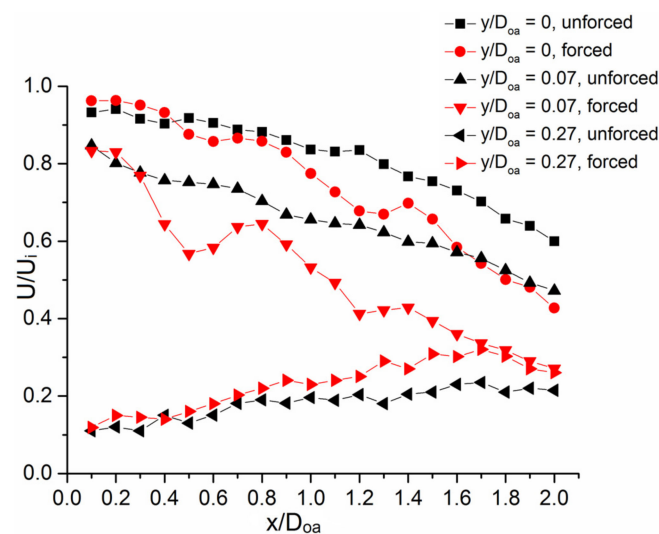

Figure 7. Velocity distribution along axial direction at different sections of nozzle B.

According to the above analysis, to further enhance the jets mixing of nozzle A, the method of increasing the momentum coefficient can be used. As an exploration research, two different methods were used to increase momentum coefficient. One was to increase the number of actuators, the combined actuators disk used above were connected in parallel and mounted on nozzle A (case 3), the measurement region moved forward 15 mm in the X axis due to the addition of combined actuators disks. The other was to use four actuators with a higher outlet velocity (case 4). Compared with Figure 2b, the potential core length in case 3 was reduced from 90 mm to 65 mm with C = 1.36% (Figure 8a), and in case 4 it was reduced to 55 mm with C = 1.47% (Figure 8b). The inner and outer shear layers were significantly thickened in case 3 and 4 compared with case1. Taking X = 40 mm as an example, along the negative direction of the Y axis, the width from the central jet velocity of 20 m/s to the annular jet velocity of 10 m/s in the inner shear layer was about 8 mm, the width from the annular jet velocity of 10 m/s to the static ambient in the outer shear layer was about 14 mm, in Figure 2b. The widths of the inner and outer shear layers of case 3 were 10 mm and 18 mm (Figure 8a). In case 4, the widths were 15 mm and 18 mm, respectively (Figure 8b). The higher the momentum coefficient, the better the mixing enhancement. Therefore, it is verified that the momentum coefficient was the most critical factor for coaxial jets mixing enhancement.
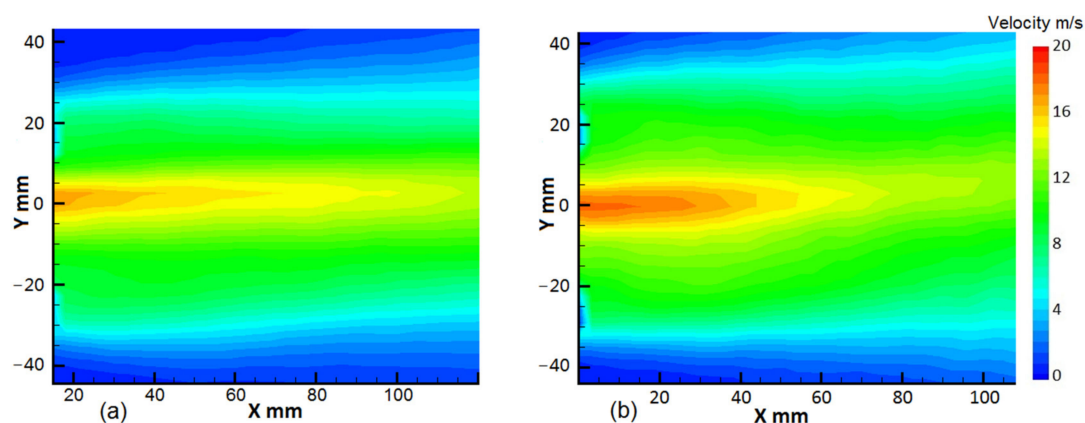
Figure 8. Time average velocity distribution of nozzle A in case 3 (**a**) and case 4 (**b**).

4. Conclusions

In this paper, the coaxial jets flow field structure and the distribution characteristics of parameters such as vorticity, streamwise velocity, radial velocity, Reynolds shear stress, and turbulence intensity with and without synthetic jets are obtained through experiments. These provided the basis for analyzing the coaxial jets mixing mechanism. Under the influence of synthetic jets, the streamwise velocity rose in the inner shear layer, then decreased on the inside of the outer shear layer and increased on the outside. The radial velocity increased significantly because the radial penetration and mixing between jets is enhanced. Because the velocity gradient became smaller and the mainstream momentum exchange range expanded, the Reynolds shear stress curve around the two peaks flattened and the span grew larger. The turbulence intensity in the outer shear layer increased significantly because the velocity pulsation in the outer shear layer became more intense. The length of the potential core significantly shortened with a higher momentum coefficient in a series of comparative experiments. Therefore, the momentum coefficient was a key factor for coaxial jets mixing enhancement.

Based on the results and discussion above, the coaxial jets mixing enhancement mechanism can be summarized. The synthetic jets penetrate into the coaxial jets and interact with it, continuously bringing vortex pairs generated by actuators into the shear layer, so that the vorticity in the shear layer greatly increased, and the streamwise vortices are enhanced. During the development of the streamwise vortices, jets were entrained and mixed. If the momentum coefficient was small, the penetration depth was small, and the streamwise vortices did not affect the mainstream center. Therefore, the mixing enhancement of the inner shear layer was not as obvious as the outer shear layer. However, as long as the momentum coefficient was large enough, the mixing of the inner shear layer can be rapidly enhanced. Therefore, by adjusting the momentum coefficient, the appropriate penetration depth and streamwise vortices influenced range can be obtained, and the mixing enhancement of the inner and outer shear layers can be controlled separately. In this way, the coaxial jets mixing enhancement control can be achieved according to the actual application situation. Future research should quantitatively analyze the relationship between the momentum coefficient and jets mixing in order to achieve accurate control of coaxial jets mixing enhancement.

Author Contributions: Experimental method: B.Z., H.L. (He Liu), and J.D.; experimental measurements: B.Z., H.L. (Hui Liu), and Y.L.; results analysis: B.Z. and H.L. (He Liu); manuscript writing: B.Z. All authors have read and agreed to the published version of the manuscript.

Institutional Review Board Statement: Not applicable.

Informed Consent Statement: Not applicable.

Data Availability Statement: The data presented in this study are available in this article.

Conflicts of Interest: The authors declare no conflict of interest.

Abbreviations

C	momentum coefficient: $4n\rho_s lwU_s^2 / \{\pi\rho_i D_i^2 U_i^2 + \pi\rho_o (D_o^2 - D_i^2) U_o^2\}$
D_c	actuator cavity diameter (mm)
D_i	inner duct outlet diameter (mm)
D_{oa}	outer duct outlet diameter of nozzle A (mm)
D_{ob}	outer duct outlet diameter of nozzle B (mm)
I	turbulence intensity
l	actuator outlet length (mm)
n	number of actuators
Re_i	center jet outlet Reynolds number
U	average velocity (m/s)
U_i	inner duct outlet velocity (m/s)
U_o	outer duct outlet velocity (m/s)
U_s	actuator outlet velocity (m/s)
u	streamwise velocity (m/s)
v	radial velocity (m/s)
w	actuator outlet width (mm)
x	axial coordinate (mm)
y	radial coordinate (mm)
ρ	density

References

1. Smith, L.; Majamaki, A.; Lam, I.; Delabroy, O.; Karagozian, A.; Marble, F.; Smith, O. Mixing Enhancement in a Lobed Injector. *Phys. Fluids* **1997**, *9*, 667–678. [CrossRef]
2. Presz, W.; Reynolds, G.; Hunter, C. Thrust Augmentation with Mixer/Ejector Systems. In Proceedings of the 40th AIAA Aerospace Sciences Meeting and Exhibit, Reno, NV, USA, 14–17 January 2002.
3. Power, G.D.; McClure, M.D.; Vinh, D. Advanced IR Suppressor Design Using a Combined CFD/Test Approach. In Proceedings of the 30th Joint Propulsion Conference and Exhibit, Indianapolis, IN, USA, 27–29 June 1994.
4. Kumar, P.A.; Rathakrishnan, E. Corrugated rightangled triangular tabs for supersonic jet control. *Proc. Inst. Mech. Eng. Part G J. Aerosp. Eng.* **2015**, *229*, 2066–2084. [CrossRef]
5. Callender, B.; Gutmark, E.; Martens, S. A PIV Flow Field Investigation of Chevron Nozzle Mechanisms. In Proceedings of the 42nd AIAA Aerospace Sciences Meeting and Exhibit, Reno, NV, USA, 5–8 January 2004.
6. Brinkerhoff, J.R.; Oria, H.; Yaras, M.I. Experimental and Computational Study of Mixing Mechanisms in an Axisymmetric Lobed Mixer. *J. Propuls. Power* **2013**, *29*, 1017–1030. [CrossRef]
7. Liu, Y.H.; Tsai, S.Y.; Wang, C.C. Effect of driven frequency on flow and heat transfer of an impinging synthetic air jet. *Appl. Therm. Eng.* **2015**, *75*, 289–297. [CrossRef]
8. Lei, W. Characteristics and mechanism of mixing enhancement for noncircular synthetic jets at low Reynolds number. *Exp. Therm. Fluid Sci.* **2018**, *98*, 731–743.
9. Zheng, X.Q. Experimental study on velocity characteristics of synthetic jet actuator. *J. Propuls. Technol.* **2005**, *26*, 504–507.
10. Luo, Z.B.; Xia, Z.X.; Liu, B. New generation of synthetic jet actuators. *AIAA J.* **2006**, *44*, 2418–2419. [CrossRef]
11. Aono, H. Straight and curved type micro dielectric barrier discharge plasma actuators for active flow control. *Exp. Therm. Fluid Sci.* **2017**, *88*, 16–23. [CrossRef]
12. Webb, N.; Samimy, M. Control of Supersonic Cavity Flow Using Plasma Actuators. *AIAA J.* **2017**, *55*, 1–10. [CrossRef]
13. Hussain, A.K.M.F.; Zaman, K.B.M.Q. Vortex pairing in a circular jet under controlled excitation. Part 2. Coherent structure dynamics. *J. Fluid Mech.* **1980**, *101*, 493–544. [CrossRef]
14. Eri, Q.; Zhang, Z.; Zhang, R.; Li, T. Numerical simulation of jet mixing enhancement using rectangular control jets. *Proc. Inst. Mech. Eng. Part G J. Aerosp. Eng.* **2019**, *233*, 111–124. [CrossRef]
15. Yang, H. Turbulent jet manipulation using two unsteady azimuthally separated radial minijets. *Proc. R. Soc. A Math. Phys. Eng. Sci.* **2016**, *472*, 2191. [CrossRef] [PubMed]
16. Muhammad, A.K.; McGuirk, J.J. Unsteady Predictions of Mixing Enhancement with Steady and Pulsed Control Jets. *AIAA J.* **2015**, *53*, 1262–1276.
17. Smith, T.D.; Cain, A.B.; Chenault, C.F. Numerical Simulation of Enhanced Mixing in Jet Plumes Using Pulsed Blowing. *J. Aircraft.* **2001**, *38*, 458–463. [CrossRef]
18. Zhou, Y.; Du, C.; Mi, J. Turbulent round jet control using two steady minijets. *AIAA J.* **2012**, *50*, 736–740. [CrossRef]

19. Kamran, M.A.; Mcguirk, J.J. Subsonic Jet Mixing via Active Control Using Steady and Pulsed Control Jets. *AIAA J.* **2011**, *49*, 712–724. [CrossRef]
20. Zdenek, T.; Vaclav, T. Annular synthetic jet used for impinging mass-transfer. *Int. J. Heat Mass Transfer.* **2003**, *46*, 3291–3297.
21. Gilarranz, J.L.; Traub, L.W.; Rediniotis, O.K. A new class of synthetic jet actuators part II application to flow separation control. *J. Fluids Eng.* **2005**, *127*, 377–387. [CrossRef]
22. Sefcovic, J.A.; Smith, D.R. Proportional aerodynamic control of a swept divergent trailing edge wing using synthetic jets. In Proceedings of the 48th AIAA Aerospace Sciences Meeting Including the New Horizons Forum and Aerospace Exposition, Orlando, FL, USA, 4–7 January 2010.
23. Slipher, C.A.; Hubbard, J.E. Exploitation of higher order membrane modes for improved synthetic jet performance. *AIAA J.* **2009**, *47*, 1388–1407. [CrossRef]
24. Chen, Y.; Liang, S.; Aung, K.; Glezer, A.; Jagoda, J. Enhanced mixing in a simulated combustor using synthetic jet actuators. In Proceedings of the 37th Aerospace Sciences Meeting and Exhibit, Reno, NV, USA, 11–14 January 1999.
25. Wang, H.; Menon, S. Fuel-Air mixing enhancement by synthetic microjets. *AIAA J.* **2001**, *39*. [CrossRef]
26. Chiekh, M.B.; Jean-Christophe, B.; Sunyach, M. Synthetic jet control for flows in a diffuser: Vectoring, spreading and mixing enhancement. *J. Turbul.* **2003**, *4*, 37–41. [CrossRef]
27. Tamburello, D.A.; Amitay, M. Active Control of a Free Jet Using a Synthetic Jet. *Int. J. Heat Fluid Flow.* **2008**, *29*, 967–984. [CrossRef]
28. Eri, Q.; Hong, L.; Li, T.; Wang, Q.; Wang, M. Numerical simulations of mixing enhancement in subsonic jet using high-momentum synthetic jets. *J. Propuls. Power* **2016**, *32*, 1095–1103. [CrossRef]
29. Hong, L.; Zhang, R.; Liu, Z. Numerical simulations of jet mixing enhancement in a round jet exhaust using SJA. *IOP Conf. Ser. Mater. Sci. Eng.* **2017**, *187*, 012013. [CrossRef]
30. Davis, S.A.; Glezer, A. The Manipulation of Large- and Small-Scales in Coaxial Jets Using Synthetic Jet Actuators. In Proceedings of the 38th Aerospace Sciences Meeting and Exhibit, Reno, NV, USA, 10–13 January 2000.
31. Ritchie, B.; Mujumdar, D.; Seitzman, J. Mixing in coaxial jets using synthetic jet actuators. In Proceedings of the 38th Aerospace Sciences Meeting and Exhibit, Reno, NV, USA, 10–13 January 2000.
32. Liu, Y.; Wang, B.; Liu, S. Investigation of Phase Excitation Effect on Mixing Control in Coaxial Jets. *J. Therm. Sci.* **2009**, *18*, 364–369. [CrossRef]